

546-33

160560

P. 12

N 93 - 27772

RESONANT TUNNELING DIODES AS SOURCES FOR MILLIMETER AND SUBMILLIMETER WAVELENGTHS

**O. Vanbésien, R. Bouregba, P. Mounaix
and D. Lippens**

Centre Hyperfréquences et Semiconducteurs U.A. CNRS N° 287
Université de Lille - 59655 Villeneuve d'Ascq Cédex - France

**L. Palmateer⁺, J.C. Pernot, G. Beaudin*
and P. Encrenaz**

Ecole Normale Supérieure 24, rue Lhomond 75231 PARIS
* Observatoire de Meudon 92195 Meudon Principal Cédex

**E. Bockenhoff⁺⁺, J. Nagle, P. Bois, F. Chevoir
and B. Vinter**

Laboratoire Central de Recherche Thomson CSF
Domaine de Corbeville 91404 Orsay Cédex - France.

ABSTRACT

High-quality Resonant Tunneling Diodes have been fabricated and tested as sources for millimeter and submillimeter wavelengths. The devices have shown excellent I-V characteristics with peak-to-valley current ratios as high as 6:1 and current densities in the range of 50-150 kA/cm² at 300 K. Used as local oscillators, the diodes are capable of state of the art output power delivered by AlGaAs-based tunneling devices. As harmonic multipliers, a frequency of 320 GHz has been achieved by quintupling the fundamental oscillation of a klystron source.

⁺ Now at IBM, Yorktown Heights ⁺⁺ at Mercedes Benz, Stuttgart

1. INTRODUCTION

Resonant Tunneling Diodes (RTD's) exhibit very strong non linearity with short time response which make them attractive in non linear applications for millimeter and submillimeter wavelengths [1]. RTD's have already demonstrated their potential for a variety of high speed/high frequency applications [2]-[5]. In this paper we report on the effort of a group of laboratories in France on these novel devices with special emphasis on local oscillators and harmonic multipliers. The fabrication procedures in a whisker contacted technology and in a microwave compatible technology suitable for monolithic integration are outlined in section 2. The DC and AC characterizations are reported in section 3 whereas the oscillator and multiplier results using the devices are described in section 4.

2. TECHNOLOGICAL PROCESS

The two types of epitaxial structures grown by molecular beam epitaxy are given in Figure 1(a) and (b). Both samples noted A and B had 17 Å - thick AlAs barriers and access regions with a stepped doping profile from $1-2 \times 10^{17} \text{ cm}^{-3}$ to $2-3 \times 10^{18} \text{ cm}^{-3}$. They differ mainly owing to the strained $\text{Ga}_{0.9}\text{In}_{0.1}\text{As}$ layers so that structure B resembles a triple well resonant tunneling structure. By placing a GaInAs well just prior the growth of the double barrier heterostructure (DBH) it is expected that the peak-to-valley current ratio (PVCR's) should be enhanced because the negative differential resistance effect involves the anticrossing of two confined states [6] [7]. In addition by placing a GaInAs well rather than a GaAs one and by a proper choice of the well width ($L_w = 40 \text{ Å}$), the ground state can be lowered in energy while keeping the excited state practically unchanged. The associated benefits are a reduction of the peak voltage and higher PVCR's [8]. Also note that structure A and B are grown on n^+ and S-I substrates respectively.

| | | |
|--------------------------|----------------------------------|--------|
| GaAs | $2 \cdot 10^{18} \text{cm}^{-3}$ | 490 nm |
| GaAs | $2 \cdot 10^{17} \text{cm}^{-3}$ | 50 nm |
| GaAs | undoped (UD) | 5 nm |
| AlAs | UD | 1.7 nm |
| GaAs | UD | 4.5 nm |
| AlAs | UD | 1.7 nm |
| GaAs | UD | 5 nm |
| GaAs | $2 \cdot 10^{17} \text{cm}^{-3}$ | 50 nm |
| GaAs | $2 \cdot 10^{18} \text{cm}^{-3}$ | 500 nm |
| n ⁺ substrate | | |

(a)

| | | |
|------------------------------------|----------------------------------|--------|
| GaAs | $3 \cdot 10^{18} \text{cm}^{-3}$ | 500 nm |
| GaAs | 10^{17}cm^{-3} | 10 nm |
| GaAs | undoped (UD) | 5 nm |
| In ₁ Ga ₉ As | UD | 5 nm |
| GaAs | UD | 0.5 nm |
| AlAs | UD | 1.7 nm |
| GaAs | UD | 0.5 nm |
| In ₁ Ga ₉ As | UD | 4 nm |

(b)

Symmetrical layers

Figure 1 : Growth sequence for the epilayer on n⁺ substrate (sample A). (a)

Sample B grown on semi-insulating substrate. (b)

The epilayers on n⁺ substrate were processed using a whisker contacted technology including patterning of Ni/GeAu layers into matrix of 3.5 μm diameter dots on the epitaxial side of the wafer and uniform deposition on the back side followed by alloying of these layers to make ohmic contacts. Mesa isolation was performed by chlorine ion beam assisted etching as shown in figure 2, using the patterned metal as a mask. As last stages some of the samples were thinned to a thickness of about 120 μm and polyimide was used to surround the diodes in order to aid whisker contact.

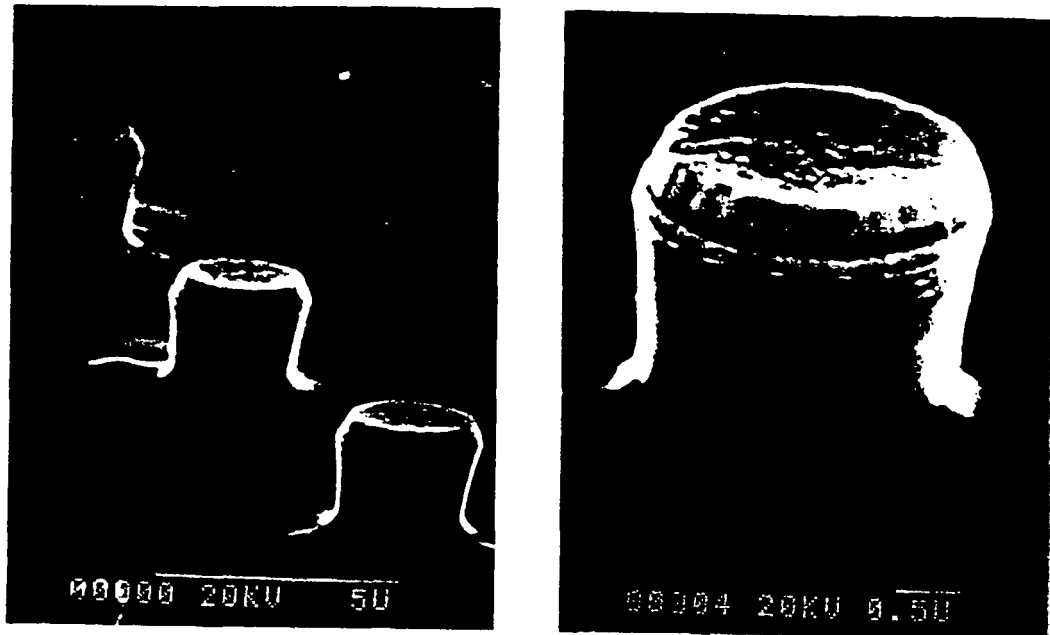


Figure 2 : SEM Photos of diodes formed by RIE.

For the epilayers on S-I substrate, the diodes were fabricated in a microwave-compatible two-step mesa technology [9]. In that case, the devices were connected to low-loss transmission lines in such a way that they can be characterized at the wafer level. Such vertically integrated devices require a means of connecting the contact on the top of the mesa to the pad of the transmission line. We thus developed two versions : (i) a dielectric assisted cross-over and (ii) an air bridge interconnection. A scanning electron micrograph of two representative devices are shown in figures 3 and 4. In figure 3 a coplanar probe configuration is apparent. Also clearly shown is the deposited strap which crosses over the mesa edges covered with Si_3N_4 layer appearing in dark. In the second version, the dielectric cross-over is replaced by an air bridge yielding a reduced parasitic capacitance. Figure 4 illustrates the technology employed with the

mushroom shaped metallization which enables one to connect small anode fingers.

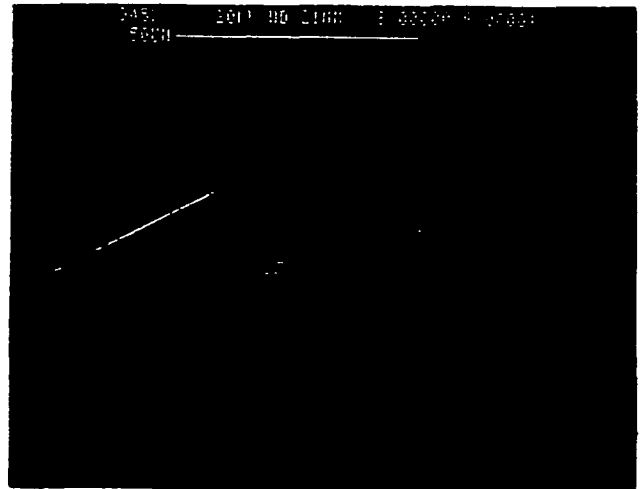
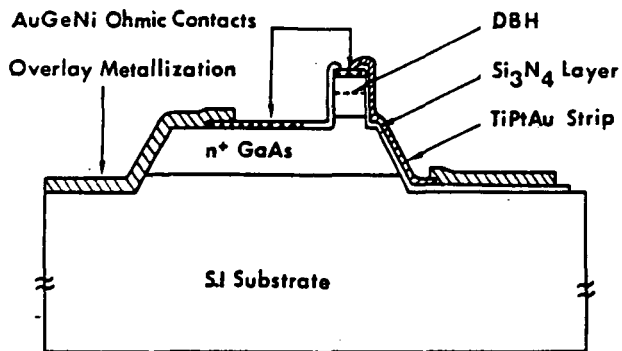


Figure 3 : Schematic cross section and SEM photo of the RTD fabricated in a planar technology.

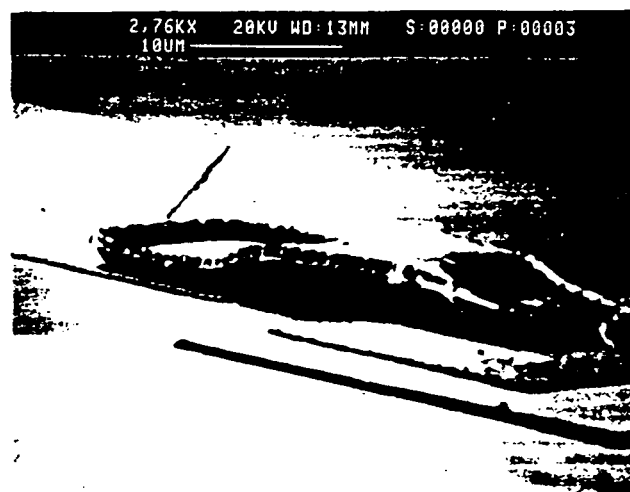


Figure 4 : SEM of a diode fabricated using air bridge techniques.

3. DC AND AC CHARACTERIZATION

Figure 5a shows a typical current voltage I-V characteristic for a GaAs/AlAs device on n+ substrate at 300K. The device exhibits a peak current of ~ 16 mA at ~ 1.8 V which corresponds to a peak current density of ~ 160 kA/cm² for a 3,5 μ m diameter diode. For larger size of the diodes, heating of the samples prevents us from achieving these densities. A typical DC characteristic for a device on SI substrate is displayed in Figure 5b. The device exhibits excellent characteristics with PVCR's as high as 6:1 along with simultaneously peak current density of 50 kA/cm² which compare favorably to the best published results [10] [11] Note also the high degree of symmetry in the I-V curve which is a good indicator of quality interfaces.

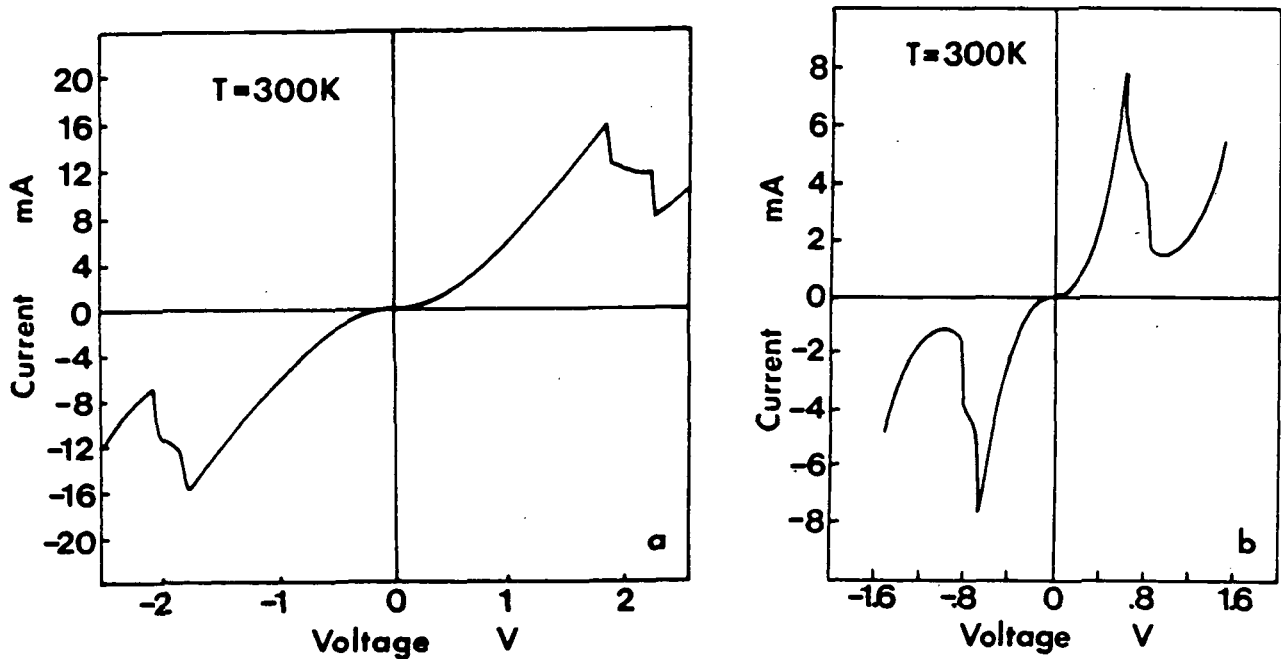


Figure 5 : Typical DC characteristics for a GaAs/AlAs device on n+ substrate (a) and for a GaInAs/GaAs/AlAs pseudomorphic device on SI substrate (b).

Following our previous work [12], on-wafer reflection gain measurements were performed between 50 MHz and 40 GHz using cascade RF probes and an 85107 A HP network analyser. Shown in Figure 6 is the one port measurement of a vertically integrated sample. The active area is $20 \mu\text{m}^2$. The diode is biased in the NDR region. Note that no de-embedding was used at this stage to correct for parasitics. For frequency evaluation, we used the equivalent circuit which consists of a single capacitor C_d with a parallel negative resistance R_d . These intrinsic lumped elements are completed by the parasitic capacitance C_p , the inductance L_p attributable to the bonding and R_s the overall series resistance. A good fit was obtained for $C_d = 36 \text{ fF}$, $R_d = -172 \Omega$, $R_s = 9 \Omega$, $L_p = 60 \text{ pH}$ and $C_p = 13 \text{ fF}$ (air-bridge technology). With this set of data derived from experiment, the cut off frequency for NDR is in excess of 100 GHz. This frequency is limited by the high impedance level needed to satisfy the stability criteria.

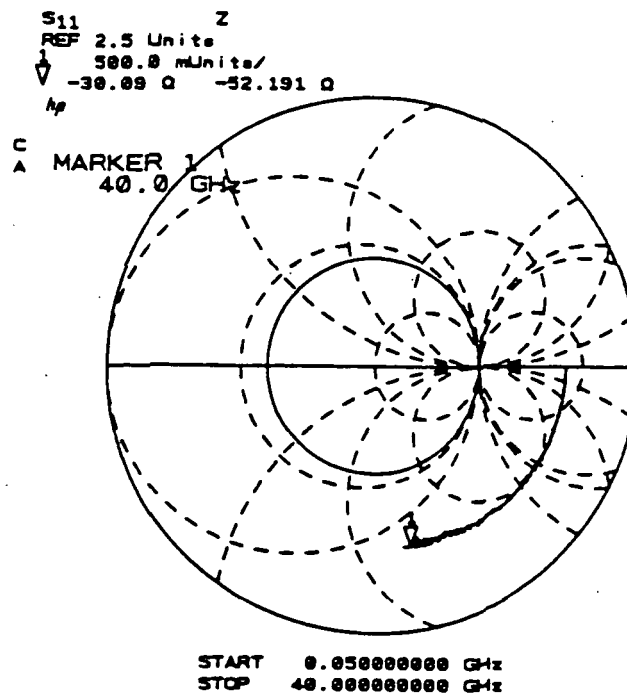


Figure 6 : One port measurement of the impedance. The bias is adjusted in the NDR region to satisfy the stability criteria.

4. OSCILLATOR AND MULTIPLIER RESULTS

The wafers on n^+ substrate were sawed into chips of $100 \times 100 \mu\text{m}^2$ and mounted in a test waveguide for measuring the oscillator power at 35 and 110 GHz. The power levels measured at 300 K with a bolometer were $36 \mu\text{W}$ at 38.6 GHz and $12 \mu\text{W}$ at 110 GHz. Referring to the oscillator results from the published literature on AlGaAs based RTD's [13] given in figure 7 the output power are state of the art results.

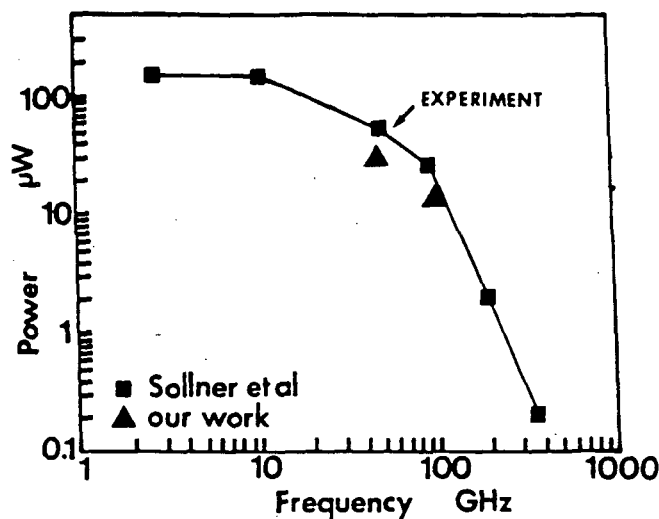


Figure 7: Experimental powers for a $4 \mu\text{m}$ diameter diode from reference [13] and results from the present work for a $3.5 \mu\text{m}$ diameter diode.

For harmonic multiplication, the samples were mounted in a commercially available multiplier mount. The measurement set up has a quasi-optical scheme and was initially developed to study reactive species of astrophysical interest [14]. The diodes were driven by a klystron at 64 GHz and, in the output path, high filters enables one to spectrally analyze the power delivered by the diode. The receiver is a helium cooled InSb detector. Figure 8 shows the power response at 3rd harmonic (192 GHz) and 5th harmonic (320 GHz). For comparison in terms of available power commercial Schottky diodes were also tested under the same

experimental conditions. It is interesting to note that equivalent performances were obtained for both types of devices by increasing the multiplication order to frequency quintupling.

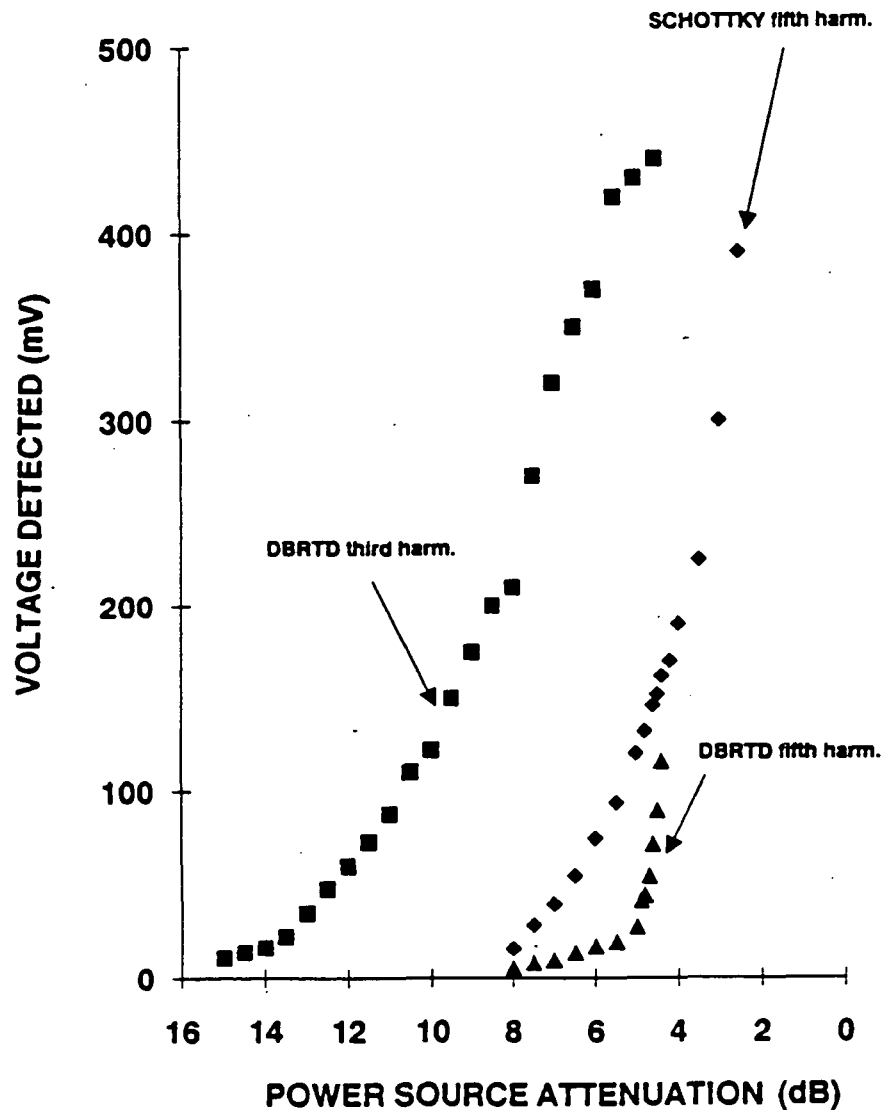


Figure 8 : Measured voltage of InSb detector against input power delivered by a klystron at 64 GHz.

In the multiplier experiment the devices were unbiased and driven in the NDR region to take advantage of multiple extrema in the current waveform. This requirement can be unfavorable especially for high threshold voltage devices when input power is limited [14]. From this viewpoint, it is clear that pseudomorphic structures with a buried well may overcome partly this difficulty. From Figure 3 it is apparent that a drastic decrease in the peak voltage 0.8 V instead of 1.8 V has been achieved by comparing structures A and B. In addition it can be noted that the PVCR's were enhanced. This suggests the superiority of these new tunneling devices for multiplication in view of the large harmonic content in the current and of the reduction of the amount of input power required to pump the diode.

5. CONCLUSION

High performance resonant tunneling diodes were successfully fabricated in a whisker contacted and in a planar technology. The RF capabilities of the diodes were demonstrated either by direct measurement of their small-signal impedance or by using them for oscillator and multiplier.

ACKNOWLEDGEMENTS

This work was supported by the Ministère de la Recherche et de la Technologie. Technical assistance of M. Bogey, J.L. Destombes and A. Lescluse with the Laboratoire de Spectroscopie Hertzienne of the Lille University is highly appreciated.

REFERENCES

- [1] T.C.L.G. Sollner, E.R. Brown and H.Q. Le, "Microwave and Millimeter-wave Resonant Tunneling Devices". Physics of Quantum Electron Devices edited by F. Capasso Springer-Verlag.
- [2] E.R. Brown, J.R. Söderstorm, CD. Parker, L.J. Mahoney, K.M. Kolvar and T.C. McGill, "Oscillations up to 712 GHz in InAs/AlSb resonant tunneling diodes". Appl. Phys. Lett. 58, pp. 2291-2293, May 1991.
- [3] A. Rydberg and H. Grönquist "Quantum well high efficiency millimeter-wave frequency tripler". Electronics Letters, Vol. 25, pp. 348-349, 1989.
- [4] P.D. Batelaan and M.A. Frerking, "A quantum well frequency multiplier with millimeter wave output". Proc. 4th Conf. Infrared Physics Zurich, pp. 527-529, 1988.
- [5] R. Bouregba, D. Lippens, L. Palmateer, E. Bockenhoff, M. Bogey, J.L. Destombes and A. Lecluse, "Frequency multiplication using resonant tunneling diode with output at submillimeter wavelengths". Electronics Lett. Vol.26, pp. 1804-1905, October 1990.
- [6] D. Thomas, F. Chevoir, E. Barbier, Y. Guldner and J.P. Vieren, "Magneto tunneling of charge build up in double barrier diodes". Proc. of 4th International Conference on Superlattices Microstructures and Microdevices 5, pp. 219-224, 1989.
- [7] P. Mounaix, O. Vanbesien and D. Lippens, "Effect of cathode spacer layer on the current-voltage characteristics of resonant tunneling diodes". Appl. Phys. Lett. 57, pp 1517-1519, October 1990.

- [8] T.P.E. Broeckaert, W. Lee and C.G. Fonstad "Pseudomorphic $\text{In}_{0.53}\text{Ga}_{0.47}\text{As}/\text{AlAs}/\text{InAs}$ resonant tunneling diodes with peak-to-valley current ratios of 30 at room temperature.
- [9] D. Lippens, E. Barbier and P. Mounaix, "Fabrication of High-Performance $\text{Al}_x\text{Ga}_{1-x}\text{As}/\text{In}_y\text{Ga}_{1-y}\text{As}/\text{GaAs}$ Resonant Tunneling Diodes using a Microwave-compatible Technology. *IEEE Electron Dev. Lett.* Vol. 12, pp. 114-116, March 1991.
- [10] R.M. Kapre, A. Madhukar, and S. Guha "Highly strained $\text{GaAs}/\text{InGaAs}/\text{AlAs}$ resonant tunneling diodes with simultaneously high peak current densities and peak-to-valley current ratios". *Appl. Phys. Lett.* 58, pp. 2255-2257, May 1991.
- [11] H. Brugger, U. Meiners, C. Wölk, R. Deufel, A. Morten, M. Rossmanith, K.V. Klitzing and R. Sauer "Pseudomorphic Two Dimensional Electron-Gas-Emitter Resonant Tunneling Devices" *Microelectronics Engineering Elsevier*, 15, pp. 663-666, 1991.
- [12] P. Mounaix, P. Bedu, D. Lippens and E. Barbier "Measurement of negative differential conductance up to 40 GHz for vertically integrated resonant tunneling diodes". *Electronics Letters* Vol. 27, pp. 1358-1359, July 1991.
- [13] E.R. Brown, T.C.L.G. Sollner, C.D. Parker, W.D. Goodhue and C. Chen. "Oscillations up to 420 GHz in GaAs/AlAs resonant tunneling diodes" *Appl. Phys. Lett.* 55, pp. 1777-1779, October 1989.
- [14] J.L. Destombes, C. Demuyneck and M. Bogey "Millimeter-wave and submillimeter-wave spectroscopy of molecular ions". *Phil. Trans. R. Soc. A* 324, pp. 147-162, 1988.